High Ionic Conductivity of Polyether-Based Network Polymer Electrolytes with Hyperbranched Side Chains

Atsushi Nishimoto, Kunihiro Agehara, Noriyuki Furuya, Toshiyuki Watanabe, and Masayoshi Watanabe*

Department of Chemistry & Biotechnology, Yokohama National University, Tokiwadai, Hodogaya-ku, Yokohama 240-8501, Japan

Received September 11, 1998; Revised Manuscript Received January 12, 1999

ABSTRACT: To achieve solvent-free polymer electrolytes with high ionic conductivity, network polymer electrolytes with hyperbranched ether side chains were synthesized. A monosubstituted epoxide monomer, 2-(2-methoxyethoxy)ethyl glycidyl ether (MEEGE), was copolymerized with ethylene oxide (EO) in the presence of 2-(2-methoxyethoxy)ethanol by base-catalyzed anionic ring-opening polymerization to semiterechelic poly[ethylene oxide-*co*-2-(2-methoxyethoxy)ethyl glycidyl ether] [P(EO/MEEGE)] oligomers with a hydroxyl terminal functional group, which was esterified with acrylic acid to a polyether macromonomer. Network polymer electrolytes were obtained by photo-cross-linking mixtures of the macromonomer, an electrolyte salt, and a photoinitiator. These polymer electrolytes consist of polyether networks with hyperbranched side chains and an electrolyte salt. The ionic conductivity changed with the molecular weight of the macromonomers and was largest when the macromonomer with molecular weight of ca. 1000 was used, although the glass transition temperature of the polymer electrolytes was nearly constant. The highest conductivity of 1×10^{-4} S cm^{-1} at 30 °C, 1×10^{-3} S cm^{-1} at 80 °C, was obtained with lithium bis(trifluoromethylsulfonyl)imide (LiTFSI) as the electrolyte salt. An electrochemically stable potential window of the network polymer electrolytes was obtained by the microelectrode technique.

Introduction

It is widely recognized that solid polymer electrolytes can be potentially applied in many solid electrochemical devices such as high-energy density batteries, electrochromic windows, and light-emitting devices.[1−4] The polymer electrolytes to be used in the devices have to satisfy several requirements, including high ionic conductivity, electrochemical stability, and good mechanical properties. Poly(ethylene oxide) (PEO) and its derivatives have been used as matrix polymers in most of studies of polymer electrolytes,[1−3] since PEO contains ether coordination sites, which assist the dissociation of salts incorporated in the polymer, as well as a flexible macromolecular structure, which promotes facile ionic transport. However, PEO-based polymer electrolytes show comparatively low ionic conductivity at ambient temperatures. The reasons for the low ionic conductivity are (a) the existence of crystalline domains, which interfere with the ionic transport, and (b) the dependence of the ionic transport on main-chain segmental motions which rapidly diminish with decreasing temperature.

There have been several approaches to solve these problems. For instance, to avoid crystallization of the matrix polymers, atactic poly(propylene oxide) (PPO) was used instead of PEO,[5] and propylene oxide was randomly copolymerized with ethylene oxide.[6] While the use of PPO and the introduction of propylene oxide can prevent the matrix polymers from crystallization, the ionic conductivity of these polymer electrolytes at room temperature is not raised to a satisfactory level. Attempts have been made to plasticize the polymers with low molecular weight solvents such as ethylene carbonate and propylene carbonate.[7−9] However, in these systems it may not be possible to avoid leakage problems.

In our previous studies[6,10−12] to achieve high ionic conductivity for solvent-free solid polymer electrolytes at ambient temperatures, we developed comblike network polymer electrolytes in which short flexible ether side chains are attached to the polyether main chain. Polymer electrolytes with short and flexible ether side chains were found to have a relatively high ionic conductivity. It was proved that the short ether side chains contribute to the fast ion transport.

In the present study, new network polymer electrolytes with hyperbranched ether side chains were synthesized by a cross-linking of macromonomers, as shown in Figure 1. It was expected that fast molecular motion of the hyperbranched side chains would contribute to fast ionic transport. To prepare the macromonomer, 2-(2-methoxyethoxy)ethyl glycidyl ether (MEEGE) was copolymerized with ethylene oxide (EO) by ring-opening anionic polymerization to obtain OH-terminated semiterechelic oligomers. These oligomers were converted to macromonomers by introducing the acrylate functionality to the ends of the oligomers. We report here the synthesis and electrochemical properties, such as ionic conductivity and electrochemical stability, for the network polymer electrolytes with the hyperbranched ether side chains. The introduction of hyperbranched structures to polyethers has been tried by several researchers,[13−15] and ionic conductivities of the polymer electrolytes based on the hyperbranched polyethers have also been reported.[13,14] A comparison of the conductivities was made between the hyperbranched polyether electrolytes, including the present electrolytes.

Experimental Section

Synthesis of Monomer. 2-(2-Methoxyethoxy)ethyl glycidyl ether (MEEGE) was synthesized by a Williamson condensation of epichlorohydrin with 2-(2-methoxyethoxy)ethanol (MEE) in the presence of tetrabutylammonium hydroxide as a phase-transfer catalyst. To the mixture of epichlorohydrin (270 g, 3

10.1021/ma981436q CCC: $18.00
Published on Web 02/11/1999

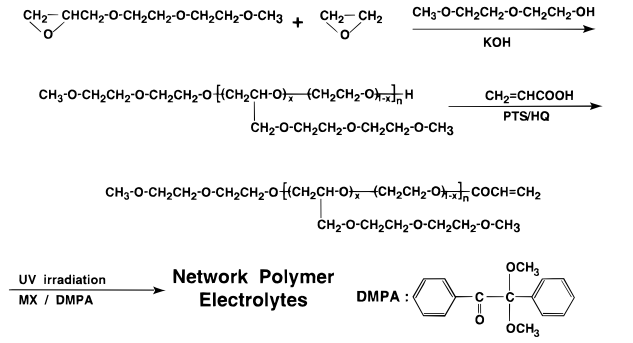

Figure 1. Synthesis of macromonomer and network polymer electrolytes.

mol) (Junsei Chemical), NaOH (120 g, 3 mol), and water (12 g, 0.67 mol), MEE (60 g, 0.5 mol) (Junsei) with dissolved tetrabutylammonium hydrogen sulfate (3.3 g, 9.7 mmol) (Kanto) was added dropwise with stirring at 40 °C. Stirring was continued for 1.5 h at 40 °C after the addition of MEE. The reaction mixture was filtered to remove excess NaOH and formed NaCl and dried with anhydrous magnesium sulfate. The crude mixture was fractionally distilled under reduced pressure several times to give a colorless liquid (26.4 g, yield 35%). Bp 90 °C/2.5 mmHg. MS: calcd for $C_8H_{16}O_4$, 176; M^+ found at $m/z = 176$. ^{1}H NMR ($CDCl_3$) δ (ppm): 2.5 (q, 1H), 2.8 (t, 1H), 3.1 (m, 1H), 3.4 (s, 3H), 3.4−3.8 (m, 10H). EO was purchased from Mitsui Toatsu Chemical (99.9%) and used without further purification.

Synthesis of Macromonomers. Into a dried 1 L autoclave were charged MEE, distilled just before use as a starting material, and 3 wt % (based on the amount of oligomers to be finally obtained) of KOH (Wako), dried under vacuum at 60 °C overnight. The autoclave was repeatedly evacuated and purged by nitrogen at 70 °C to remove water and to obtain the potassium alkoxide. An approximately 20 g portion of the mixture of MEEGE, distilled just before use, and EO ([MEEGE]/[EO] = 15/85) was added several times into the autoclave at 120 °C. After the final addition of the mixture, stirring was continued for 2 h at 120 °C. After the reaction mixture was cooled to 50 °C, an equivalent amount of water was added to the autoclave to convert the potassium alkoxide to KOH. After neutralization with sulfuric acid and desalting, the reaction mixture was dried under high vacuum at 120 °C to obtain pale-yellowish viscous liquids of OH-terminated oligomers (Figure 1). These oligomers were characterized by ^{1}H NMR, IR, GPC, and hydroxyl group titration as mentioned below.

Acrylic acid (Wako), *p*-toluenesulfuric acid (PTS, Kanto) as a catalyst, and hydroquinone (HQ, Wako) as a polymerization inhibitor were added to solutions of the OH-terminated oligomers in toluene (Wako). Esterification proceeded by removing the formed water as the toluene azeotrope at 125 °C for 10 h. The excess acrylic acid, PTS, and HQ were neutralized by NaOH aqueous solutions and then desalted. The reaction mixture was extracted by toluene after filtration, and toluene was evaporated under vacuum to obtain a pale-yellowish viscous liquid (Figure 1). Finally, all the macromonomers were dried under reduced pressure at 50 °C (the water content <20 ppm) and kept under argon in a dry glovebox (VAC, $[O_2] <$ 0.1 ppm, $[H_2O] <$ 1 ppm). The degree of acrylation was determined by saponification and ^{1}H NMR, as described below.

Preparation of Network Polymer Electrolytes. Lithium bis(trifluoromethylsulfonyl)imide (LiTFSI) (kindly supplied by IREQ), lithium perchlorate ($LiClO_4$) (Wako), lithium tetrafluoroborate ($LiBF_4$) (Tomiyama Chemical)), lithium hexafluorophosphate ($LiPF_6$) (Tomiyama), lithium trifluoromethanesulfonate ($LiCF_3SO_3$) (Wako), sodium trifluoromethanesulfonate ($NaCF_3SO_3$) (Wako), and potassium trifluoromethanesulfonate (KCF_3SO_3) (Wako) were used as electrolyte salts for the network polymer electrolytes. All the alkali metal salts were dried under high vacuum at 120 °C and stored in the dry glovebox. Weighed amounts of the salt, the macromonomer, and 2,2-dimethoxy-2-phenylacetophenone (Ciba Geigy, 0.05 wt % based on the macromonomer) photoinitiator were mixed together in the glovebox to homogeneous viscous solutions. These were spread between two glass plates separated by poly(tetrafluoroethylene) (PTFE) spacers and were irradiated with UV light (250 W super-high-pressure Hg lamp, Ushio Electric) for 5 min to obtain flexible polymer electrolyte films (Figure 1).

Characterization of Macromonomers and Network Polymer Electrolytes. IR spectra were measured by using a Shimadzu IR-415 spectrophotometer. The NaCl plate method was used for the characterization. A JEOL-EX270 was used to obtain NMR spectra by using $CDCl_3$ as the solvent.

The molecular weight of the oligomers was determined by the titration of the terminal hydroxyls. An excess of a mixture of acetic anhydride and pyridine was added to a weighed amount of the oligomers, and the reaction was continued at the reflux temperature for 30 min. Water was added to the solution to hydrolyze the excess acetic anhydride, and the solution was titrated with 1 N KOH.

The molecular weight of the OH-terminated oligomers was also determined by gel permeation chromatography (Shimadzu SCL-6A) equipped with a refractive index detector (Shodex RI SE-51). A JASCO Megapack GEL 201 column was employed and calibrated by using poly(ethylene glycol) standard samples (Tosoh).

The degree of acrylation of the macromonomers was determined by saponification. A NaOH−ethanol solution was added to a weighed amount of the macromonomer. After hydrolysis at 50 °C for 1 h, the excess NaOH was titrated with HCl.

The course of the photo-cross-linking reaction of the macromonomers was evaluated by measuring the gel fractions. The network polymers were prepared by irradiating with UV light for different periods, and the unreacted macromonomer was extracted with methanol.

Differential scanning calorimetry (DSC) was carried out on a Seiko Instruments DSC 220C under nitrogen atmosphere. The vacuum-dried samples were sealed in Al pans in the dry glovebox. The DSC thermograms were recorded during the programmed heating (10 K/min) after quenching from 120 to −120 °C.

Electrochemical Measurements. Alternating current impedance was measured with a computer-controlled Hewlett-Packard 4192A LF impedance analyzer over the frequency range from 5 Hz to 13 MHz at an amplitude of 10 mV. The polymer electrolyte films were cut into disks of 13 mm diameter. The disks were placed between two stainless steel blocking electrodes and were sealed in PTFE containers as in our previous report.[16] All ionic conductivities were measured in a thermostated oven from 100 to −10 °C.

The combined use of complex impedance and potentiostatic polarization was made with the impedance analyzer, a dc voltage source (Advantec R6142), and a zero-shunt ammeter (Hokuto Denko HM-103) to determine the apparent transference number of Li^+ ion in the polymer electrolytes. The polymer electrolytes sandwiched between metallic lithium electrodes were sealed in the PTFE containers. The dc polarization at 10 mV was conducted at 60 °C to record the change in the polarization current, after measuring the complex impedance.

The electrochemical stability was investigated by cyclic voltammetry with a three-electrode microcell consisting of a Ni working electrode (50 μm diameter) and Ag and Pt electrodes (0.4 mm diameter) as reference and counter electrodes, respectively. The details of fabrication of the microcell have been previously described.[17] Cyclic voltammetry was carried out at a sweep rate of 10 mV s^{-1} at 60 °C under an Ar atmosphere.

Results and Discussion

Preparation of Macromonomers and Network Polymer Electrolytes. Seven macromonomers, with different molecular weight, were synthesized by anionic copolymerization of MEEGE with EO, followed by esterification with acrylic acid, as shown in Table 1.

Table 1. Preparation and Characterization of P(EO/MEEGE)

	monomer in feed	OH-terminated prepolymer			acrylated macromonomer	network polymer
abbreviation	[EO]/[MEEGE]	M_n[a]	M_w/M_n[b]	[EO]/[MEEGE][c]	deg of acrylation (%)[d]	T_g (°C)
P(EO/MEEGE)470	85/15	470, 460	1.08	85/15	100, 90	−68.0
P(EO/MEEGE)500	85/15	500, 490	1.08	85/15	94, 100	−68.9
P(EO/MEEGE)710	85/15	710, 660	1.07	85/15	98, 100	−68.6
P(EO/MEEGE)850	85/15	860, 870	1.07	85/15	87, 78	−71.3
P(EO/MEEGE)990	85/15	990, 830	1.11	85/15	97, 100	−68.7
P(EO/MEEGE)1500	85/15	1500, 1160	1.53	85/15	99, 100	−67.4
P(EO/MEEGE)2000	85/15	2000, −		85/15	100, 94	−66.7

[a] Left: determined from hydroxyl group titration. Right: determined from GPC. [b] Determined from GPC. [c] Determined from ^{1}H NMR and M_n from hydroxyl group titration. [d] Left: determined from saponification value. Right: determined from ^{1}H NMR.

MEEGE could be copolymerized with EO in the presence of the potassium alkoxide. Progress of the polymerization was monitored by the change of the monomer vapor pressure. Since the reactivity of MEEGE was lower than that of EO, a small portion of the mixture of MEEGE and EO was injected into the autoclave at half-hour intervals to introduce MEEGE randomly into the copolymers. The pressure decreased to an original value within 15 min after introducing the monomer mixture. The agreement between the number-average molecular weight (M_n) determined by both of the hydroxyl group titration and GPC (Table 1) shows that the anionic polymerization using MEEGE and EO proceeds quantitatively to P(EO/MEEGE) with a OH group at one end. The molecular weight distributions (M_w/M_n) determined from GPC are relatively narrow (1.07−1.53). The ^{1}H NMR spectrum of the OH-terminated oligomer of P(EO/MEEGE)500, shown in Figure 2A, exhibits peaks at $\delta = 3.38$, 3.5−3.8, and 3.85−4.00, which can be assigned to OCH_3, the other methylene and methyne protons, and alcoholic protons, respectively. The copolymer compositions of P(EO/MEEGE) were estimated by combination of the ^{1}H NMR spectrum and M_n estimated by the hydroxyl group titration. The ratios of the area of the peaks corresponding to the methoxy protons (I_{OCH_3}) and the other protons (I_{others}), and M_n are

$$I_{OCH_3}/I_{others} = (3 + 3nx)/(8 + 8nx + 4n)$$

$$M_n = n[44(1 - x) + 176x] + 120$$

where n and x are the degree of polymerization and the copolymer composition of MEEGE in the P(EO/MEEGE), respectively, as shown in Figure 2A. Good agreement of the calculated MEEGE compositions of P(EO/MEEGE) by using the above relations and the expected values ([EO]/[MEEGE] = 85/15 in the feed) indicates quantitative anionic copolymerization of MEEGE with EO by using the potassiun alkoxide as an initiator.

The ^{1}H NMR spectrum of the acrylated macromonomer of P(EO/MEEGE)500 shows new peaks at $\delta = 5.8$−6.5, assignable to the protons of the acrylate group, as shown in Figure 2B. The degrees of acrylation estimated by both the saponification and ^{1}H NMR are similar and approximately quantitative (Table 1).

The photo-cross-linking reaction of the acrylated macromonomers occurred in the presence of the photoinitiator. Figure 3 shows the gel fraction for the P(EO/MEEGE)850 network polymer as a function of UV irradiation time; all of the polymer is cross-linked within 120 s of UV irradiation. On the other hand, only 85% of the acrylates react during 120 s of UV irradiation (Figure 4) as determined by monitoring the absorbance at 1633 cm^{-1}, attributable to the C═C stretching vibration mode, in the IR spectra. Since 95% of the acrylates reacted after irradiation for 5 min, such polymer networks were used for the following electrochemical experiments.

Although the photo-cross-linking reaction of the monoacrylated macromonomer is unexpected, the cross-linking was very fast (Figure 3), possibly due to the presence of a small amount of diacrylated macromonomer in the monoacrylated macromonomer. It is well-known that a trace amount of residual water reacts with EO in the presence of a base to form ethylene glycol. The ethylene glycol reacts with the monomers to yield the P(EO/MEEGE) diols whose molecular weights are approximately twice as high as those of P(EO/MEEGE) mono-ols. Figure 5 shows a GPC elution profile of the OH-terminated oligomer (P(EO/MEEGE)710) as a typical example. The profile is unimodal, and neither satellite peak nor shoulder is observed at the elution time corresponding to the molecular weight twice as high as the peak molecular weight. However, a trace of the diacrylated macromonomer may still be present. Photolysis of the ether structure would be a supplementary reason for the cross-linking. Lerner et al. reported[18,19] photo-cross-linking of polymer electrolytes based on poly[oxymethylene-*co*-oligo(oxyethylene)](PEM) in the presence of a photoinitiator. They assume, referring to a report on the photolysis of an ether,[20] that photo-cross-linking of PEM occurs due to the reaction between radical precursors, which are formed by photolysis of the ether structure, followed by a hydrogen transfer. The rapid cross-linking of the present macromonomers may have been caused by both these factors.

Temperature Dependence of Ionic Conductivity. All the polymer electrolytes obtained were completely amorphous, reflecting the random introduction of MEEGE into EO sequence in the macromonomers, as determined by DSC. Figure 6A shows the temperature dependence of ionic conductivity for the P(EO/MEEGE)850 network polymer electrolytes complexed with LiTFSI, which exhibits the highest ionic conductivity. The ionic conductivity of the polymer electrolyte ([Li]/[O] = 0.04) reaches ca. 10^{-3} S cm^{-1} at 80 °C and ca. 10^{-4} S cm^{-1} at 30 °C, exceptionally high values for solvent-free polymer electrolytes. To exclude the possibility that unreacted macromonomers function as plasticizers to enhance the conductivity, the following experiments were carried out. The network polymer films obtained by photo-cross-linking reaction in the absence of the salt were extracted by methanol to remove unreacted macromonomer and then soaked in a methanol solution of LiTFSI. The methanol was then evaporated to obtain the polymer electrolyte films,

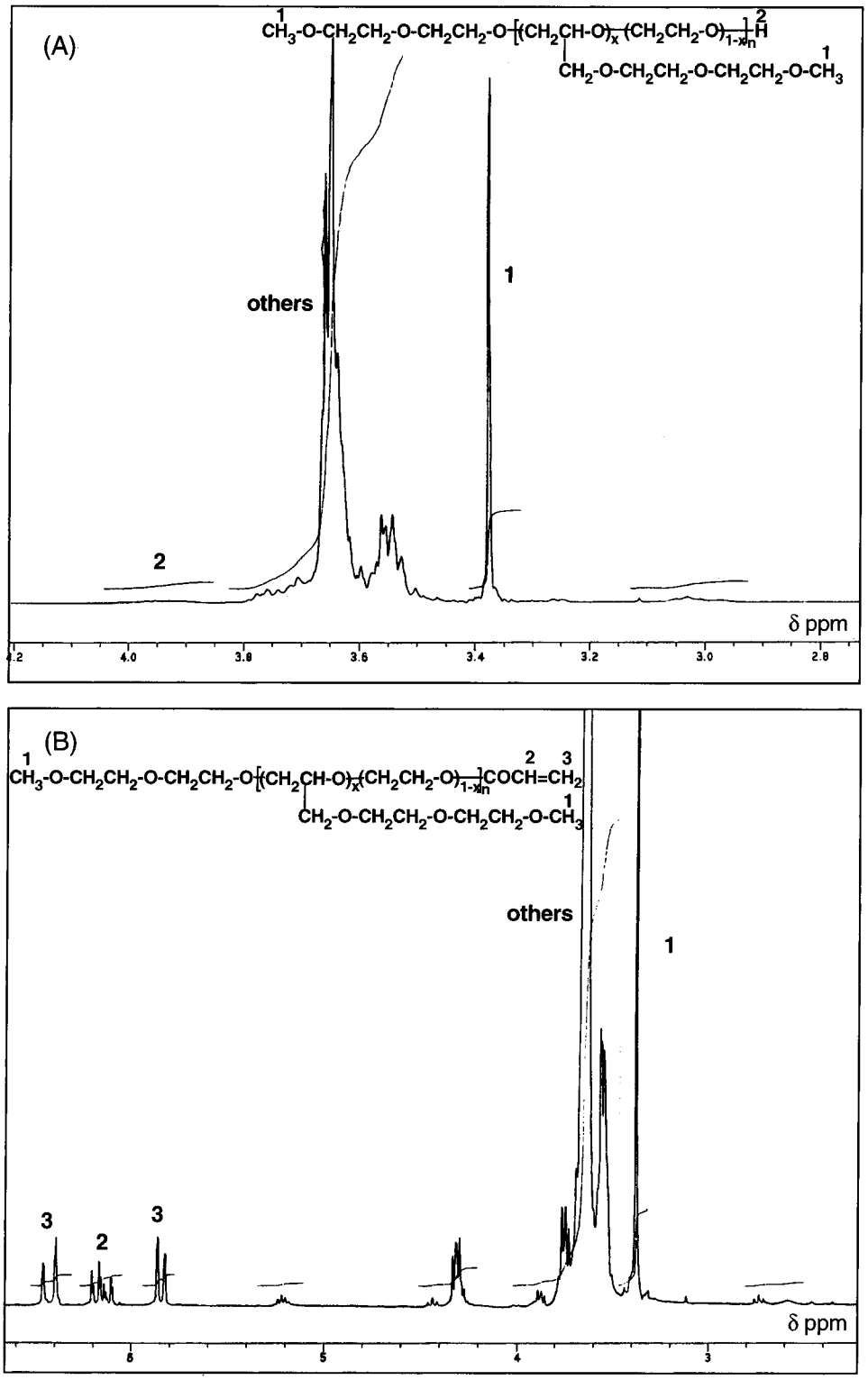

Figure 2. NMR spectrum ($CDCl_3$, δ from TMS) of OH-terminated prepolymer (A) and acrylated macromonomer (B) for P(EO/MEEGE)500.

which could not contain unreacted macromonomers. Figure 6B shows the temperature dependence of the ionic conductivity for such P(EO/MEEGE)850 polymer electrolytes complexed with LiTFSI ([Li]/[O] = 0.04). Although the ionic conductivities are different depending on the UV irradiating time, i.e., the polymer electrolyte prepared by the UV irradiation for 100 s exhibits a little higher ionic conductivity than that of the polymer electrolyte prepared by irradiation for 5 min, the ionic conductivities of the polymer electrolytes prepared by two different methods (compare parts A and B of Figure 6) are almost identical. Thus, the high conductivity seen in Figure 6 is not caused by plasticization by the unreacted macromonomers, and the photocross-linking of the macromonomers in the presence of a dissolved salt gives completely cross-linked polymer electrolytes.

The temperature dependence of ionic conductivity for the polymer electrolytes can be represented well by a Williams−Landel−Ferry (WLF) type equation:

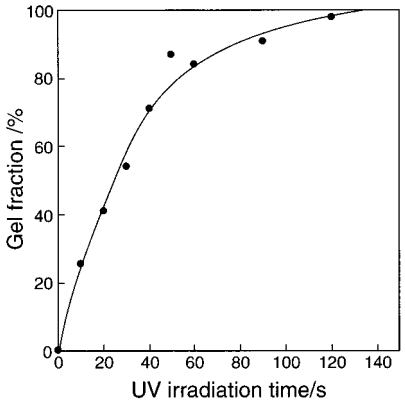

Figure 3. Gel fraction for P(EO/MEEGE)850 network polymer plotted against UV irradiation time.

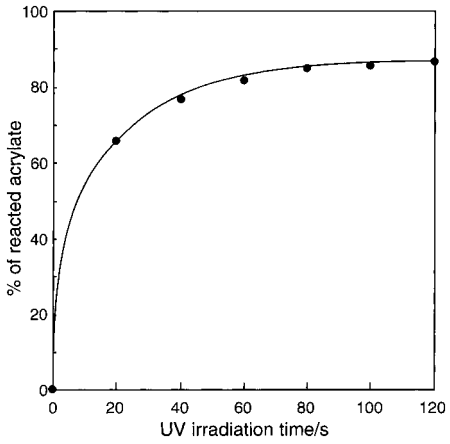

Figure 4. Reacted acrylate in P(EO/MEEGE)850 macromonomer determined from absorbance at 1633 cm^{-1} as a function of UV irradiation time.

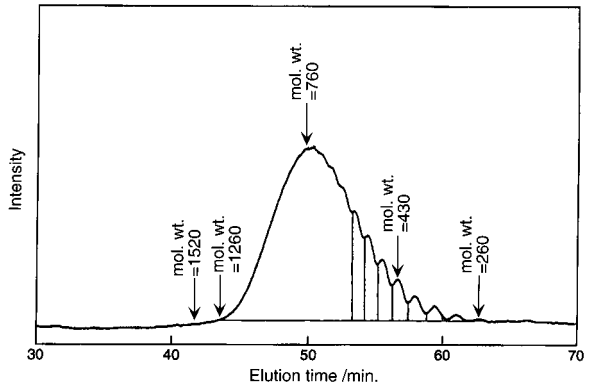

Figure 5. GPC chromatogram of OH-terminated prepolymer (P(EO/MEEGE)710).

$$\log[\sigma(T)/\sigma(T_0)] = [C_1(T - T_0)]/[C_2 + (T - T_0)]$$

where $\sigma(T)$ and $\sigma(T_0)$ are ionic conductivities at T and a reference temperature ($T_0 = T_g + 50$ K in this study), respectively, and C_1 and C_2 are constants. The resulting WLF parameters for the P(EO/MEGE)850 network polymer electrolytes complexed with LiTFSI are typically shown in Table 2. The solid lines in Figure 6A are calculated values from the WLF type equation and the parameters shown in Table 2.

Salt Concentration and Ionic Conductivity. Figure 7 shows ionic conductivity at 30 °C (upper) and T_g (bottom) for the network polymer electrolytes based on P(EO/MEEGE)500 and 990 complexed with LiTFSI at several concentrations. The ionic conductivity increases, passes a maximum at [Li]/[O] = 0.04, and then decreases with increasing salt concentration. On the other hand, T_g increases linearly with increasing salt concentration. The ionic conductivity is in proportion to the product of the number of charge carriers and their mobility. The increase in the T_g can be ascribed to the inter- and intramolecular coordination of ether dipoles with the charge carriers, i.e., dissociated ions, which may act as transient cross-linking points in the polymer electrolytes. The increase in the T_g decreases segmental motion of the matrix polymer, which directly reduces the ionic mobility. In contrast, the number of charge carriers may increase with increasing salt concentration. The ionic conductivity maxima seen in Figure 7 are assumed to be caused by these two opposite effects on conductivity.

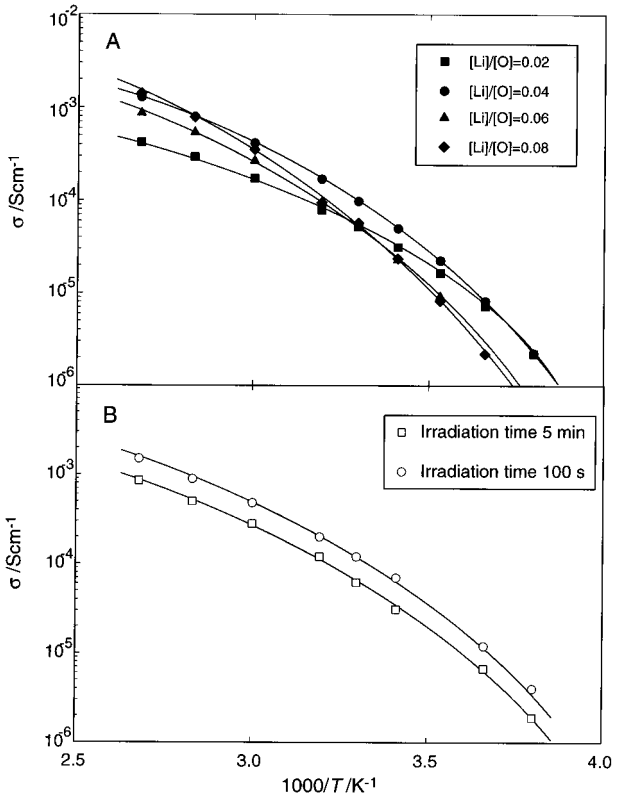

Figure 6. Arrhenius plots of ionic conductivity for P(EO/MEEGE)850 network polymer electrolytes complexed with LiTFSI: A, at different salt concentrations; B, the network polymers were extracted with methanol, followed by doping with LiTFSI at [Li]/[O] = 0.04.

Table 2. Glass Transition Temperatures and WLF Parameters for P(EO/MEEGE)850 Network Polymer Electrolytes Containing LiTFSI

[Li]/[O]	T_g/°C	C_1	C_2/°C	$\sigma(T_0)$/S cm^{-1}
0.02	−67.2	4.01	54.10	7.46×10^{-7}
0.04	−57.0	4.32	72.61	3.42×10^{-6}
0.06	−48.4	4.38	79.27	3.50×10^{-6}
0.08	−44.4	4.76	86.53	4.88×10^{-6}

To confirm the validity of the above assumption, the $\sigma(T_0)$ values are calculated by using the WLF parameters which fit the temperature dependence of the ionic conductivity. According to the conventional free volume theory,[21] the fractional free volume in amorphous polymers increases linearly with $T - T_g$. The reference temperature, T_0, would correspond to an iso-free volume state. The fact that the temperature dependence of ionic

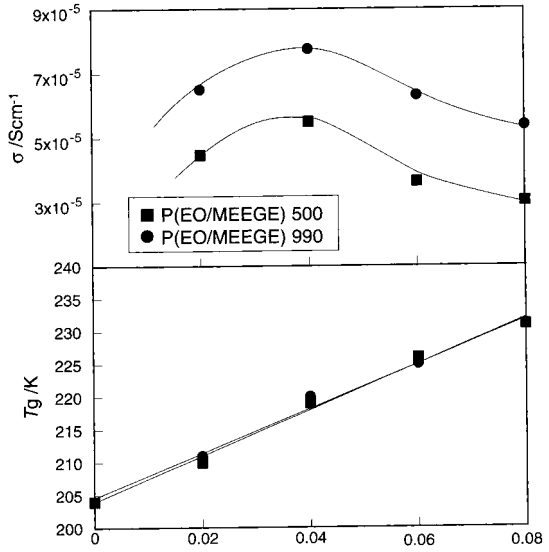

Figure 7. Ionic conductivity at 30 °C (upper) and T_g (bottom) for P(EO/MEEGE)500 and P(EO/MEEGE)990 network polymer electrolytes as a function of LiTFSI concentration.

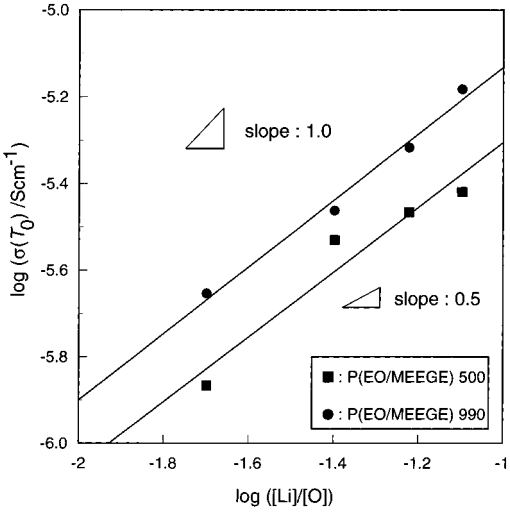

Figure 8. Ionic conductivity [$\sigma(T_0)$] at a reference temperature ($T_0 = T_g + 50$ °C) as a function of LiTFSI concentration.

conductivity is expressed by a WLF type equation indicates that the ionic conductivity change is dominated by the ionic mobility change and that the mobility change is rationalized by the free volume theory. Thus, the $\sigma(T_0)$ values can be considered to be the ionic conductivity values at an isomobility state. Figure 8 shows a bilogarithmic plot of $\sigma(T_0)$ against the concentration of [Li]/[O]. In contrast to the isothermal conductivity change as a function of the salt concentration, seen in Figure 7, the $\sigma(T_0)$ increases with increasing salt concentration. This implies that the increase in $\sigma(T_0)$ reflects an increase in the number of charge carriers. In Figure 8, the experimentally determined slopes of the plots are compared with a slope of 1.0 corresponding to complete dissociation of the incorporated salt in the polymer electrolytes, and a slope of 0.5 is expected when ion pair formation is predominant.[22] The experimental slopes of ca. 0.75 are intermediate. It is known that LiTFSI is highly dissociated even in organic solvents.[23−25] Our analysis on the conductivity change at the isomobility state indicates that the equilibrium between ion pairs and free ions, without further aggregations, is predominant for LiTFSI in the polyether networks.

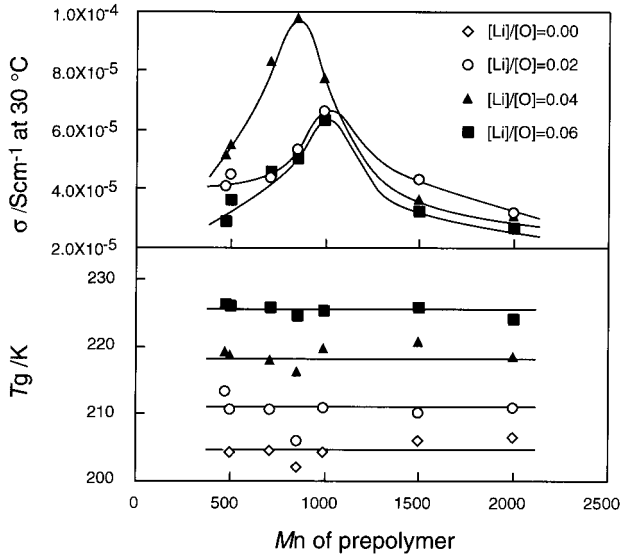

Figure 9. Ionic conductivity at 30 °C (upper) and T_g (bottom) of P(EO/MEEGE) network polymers complexed with LiTFSI plotted against M_n of OH-terminated prepolymers.

Effect of Macromonomer Molecular Weight on Ionic Conductivity. Figure 9 shows ionic conductivity at 30 °C (upper) and T_g (bottom) of the P(EO/MEEGE) network polymers complexed with LiTFSI as a function of number-average molecular weight (M_n) of the hydroxy-terminated P(EO/MEEGE). M_n would correspond to an average length of the hyperbranched side chains in the network copolymers. The ionic conductivity passes through a maximum at M_n of ca. 800−1000, although T_g is insensitive to M_n. The difference of ionic conductivity is caused by the difference of the number of charge carriers and/or their mobility. In the conventional free volume theory, the ionic mobility at 30 °C would not change greatly, since T_g of the network polymer electrolytes is independent of M_n. This consideration suggests that the conductivity maxima are caused by the maxima of the number of carrier ions. However, it is quite unlikely that the dissociation of the lithium salt differs as much as seen in the change in the conductivity, because the chemical structure of the macromonomers is identical. The conductivity maxima must then be caused by the difference of the ionic mobility with the change in the length of hyperbranched side chains in the network polymers. The local mobility of the hyperbranched side chain does not affect T_g of the network polymer electrolytes, but it would be largest at a certain chain length, which causes the conductivity maxima seen in Figure 9.

Here, one may encounter inconsistency that a constant $T-T_g$ represents an isomobility state for the effect of salt concentration in an identical network polymer (Figure 8) but does not represent it for the effect of the hyperbranched side chain lengths (Figure 9). Since temperature dependence of conductivity for all the polymer electrolytes in this study can be described by the WLF type equation with similar C_1 and C_2 parameters, as shown in Table 2, one cannot doubt that the conductivity change is dominated by the ionic mobility change, which is essentially governed by $T-T_g$. However, $\sigma(T_0)$ or σ at a constant $T-T_g$ changes in each network polymer due to the difference in the ionic mobility that can be enhanced by the presence of the hyperbranched side chains of optimized lengths. This consideration is also confirmed by the fact in Figure 8

Table 3. Ionic Conductivity and Glass Transition Temperatures of P(EO/MEEGE)710 Network Polymer Electrolytes Complexed with Several Different Salts ($[M^+]/[O] = 0.04$)

		σ/S cm^{-1}	
salt	T_g (°C)	at 80 °C	at 30 °C
LiTFSI	−54.4	6.9×10^{-4}	8.3×10^{-5}
$LiClO_4$	−49.0	2.9×10^{-4}	2.8×10^{-5}
$LiCF_3SO_3$	−53.8	1.7×10^{-4}	2.4×10^{-5}
$LiBF_4$	−51.6	1.7×10^{-4}	2.3×10^{-5}
$LiPF_6$	−49.5	1.9×10^{-4}	1.5×10^{-5}
$NaCF_3SO_3$	−54.7	3.2×10^{-4}	3.6×10^{-5}
KCF_3SO_3	−54.2	3.8×10^{-4}	3.8×10^{-4}

that the absolute magnitude of $\sigma(T_0)$ is larger for the P(EO/MEEGE)990 network polymer electrolytes.

Effects of Salt Structure and Network Architecture on Ionic Conductivity. The ionic conductivity was measured for the polymer electrolytes complexed with both LiTFSI and other alkali metal salts. A comparison of the ionic conductivity and T_g for the polymer electrolytes complexed with different alkali metal salts is given in Table 3. The conductivity of the polymer electrolyte complexed with LiTFSI is significantly higher than that complexed with other lithium salts. This high conductivity is attributed to the particular characteristics of $(CF_3SO_2)_2N^-$ ($TFSI^-$), as described in many studies.[26,27] The $TFSI^-$ has a highly delocalized anionic charge, flexible structure, and large ionic radius. These characteristics may be reflected by facile ionic dissociation of LiTFSI and by weak interaction of $TFSI^-$ with polyether solvent dipoles. In fact, high dissociation of LiTFSI in the network polymers is also indicated in Figure 8, and the weak interaction is confirmed by the lowest T_g in the polymer electrolytes complexed with lithium salts (Table 3). The effect of cationic species on the ionic conductivity was explored by using triflate salts. The conductivity follows the order of $KCF_3SO_3 > NaCF_3SO_3 > LiCF_3SO_3$, whereas T_g of the polymer electrolytes is almost the same. The conductivity difference may be caused by the difference in the degree of dissociation of these triflate salts.

The ionic conductivities of the present polymer electrolytes, reaching 10^{-4} S cm^{-1} at room temperature, are rather high even if a comparison of ionic conductivities is made in the polymer electrolytes of hyperbranched polyethers. Marchese et al.[13] reported that the polymer electrolytes based on the chain-extended comblike polyepoxides showed conductivities up to 10^{-4} S cm^{-1} at room temperature, which is close to the present results. Hawker et al.[14] prepared hyperbranched poly(ethylene glycol)s (PEGs) by condensation of AB_2 macromonomers, and a conductivity of 10^{-5} S cm^{-1} was obtained when they were complexed with a lithium salt. The former hyperbranched polyethers are copolymers of PEG monoglycidyl ether with PEG diglycidyl ether by anionic polymerization and have highly flexible structures, like the present network polymers, whereas the latter hyperbranched polyethers contain dihydroxybenzoate structure at each branching point. It is suggested that the total chain flexibility as well as the hyperbranched structures greatly influences the ionic conductivities.

Apparent Li^+ Transference Number and Potential Window. For binary electrolyte systems including polymer electrolytes, it is very important to investigate the proportion of the currents transported by each ionic species. For polymer electrolytes complexed with lithium salts, the proportion of the current transported by lithium ions, i.e., lithium ion transference number (t_{Li^+}), is one of the most significant parameters that determine performance of the polymer electrolytes when they are applied in electrochemical devices. However, since ionic association frequently takes place in such low polar media as polyethers, reliable methods to determine t_{Li^+} in polymer electrolytes has not been established. In this study, apparent t_{Li^+} was estimated for the network polymer electrolytes complexed with LiTFSI by the combination of ac impedance measurement and potentiostatic polarization measurement. A transference number is given by

$$t_{Li^+} = R_b/[V/I(\infty) - R_i]$$

where R_b and R_i are bulk resistance and interfacial resistance, respectively, obtained from the complex impedance measurements, and $I(\infty)$ and V are steady-state limiting current and applied potential, respectively, obtained from the potentiostatic polarization measurements. This method yields the real transference number if the electrolyte salts are completely dissociated and there are no mobile ion pairs.[28,29] The apparent t_{Li^+} values of 0.08 for P(EO/MEEGE)850, 0.05 for P(EO/MEEGE)1500, and 0.08 for P(EO/MEEGE)2000 network polymer electrolytes ($[Li]/[O] = 0.06$) were low, as has been reported in polyether-based polymer electrolytes complexed with LiTFSI.[6] Stronger interaction between polyether dipoles and lithium ions than that between those and the anions, due to high donor number of polyether oxygen, may cause to limit the cationic transport, whereas the anionic motion occurs rather freely. Prud'homme et al. recently reported apparent t_{Li^+} values, defined as the ratio (σ_{eff}/σ) of cationic effective conductivity over global conductivity, for amorphous polyether electrolytes containing several different salts.[30] Under the assumption of an ideal electrolyte containing either ion pairs or triple ions, the apparent t_{Li^+} value was estimated by theoretical modeling and was found to depend on association constants of salts and relative diffusivity of Li^+ to those of anions, ion pairs, and ion triplets. They also found experimentally very low apparent t_{Li^+} values for the LiTFSI electrolytes and concluded that LiTFSI should have a quite low association constant in the polymer electrolytes and that the diffusivity of TFSI anion is much faster than that of Li^+. These results and consideration are consistent with our study.

Figure 10 shows a cyclic voltammogram at a Ni microelectrode of 25 μm diameter at 60 °C for the P(EO/MEEGE)850 network polymer electrolyte complexed with LiTFSI at $[Li]/[O] = 0.06$, as a typical example. The anodic limit is irreversible oxidation observed at ca. 2.5 V vs Ag. On the other hand, deposition and stripping processes of Li/Li^+ are clearly seen at ca. 3 V vs Ag, though small cathodic peaks appear in the cathodic scan.

Conclusions

The network polyethers with hyperbranched ether side chains were synthesized for the matrixes of polymer electrolytes from the P(EO/MEEGE) macromonomers. The polymer electrolytes complexed with LiTFSI exhibit comparably high ionic conductivities of 10^{-4} S cm^{-1} at 30 °C and 10^{-3} S cm^{-1} at 80 °C in the absence of any

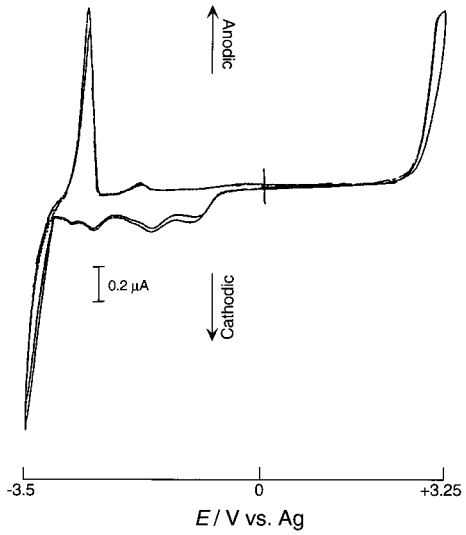

Figure 10. Cyclic voltammogram at Ni microelectrode (25 μm diameter) at 60 °C for P(EO/MEEGE)850 network polymer electrolyte complexed with LiTFSI ([Li]/[O] = 0.06).

plasticizer. The ionic conductivity changes depending on the macromonomer molecular weight, which corresponds to the length of the hyperbranched side chains, although no change in the T_g values occurs. The conductivity passes a maximum for the network polymer electrolytes from P(EO/MEEGE) macromonomer with molecular weight of ca. 1000. This maximum may be caused by the ionic mobility maximum due to local motion of the hyperbranched side chains. Fast ion transport by fast side chain motion is a new concept to design highly conductive polymer electrolytes. LiTFSI in the network polymers must be highly dissociated, as reflected by the dependence of the conductivity on salt concentration in the iso-free-volume state as well as by the apparent t_{Li^+} values.

Acknowledgment. This research was supported in part by Grant-in-Aid for Scientific Research (#10650878) and that on Priority Area "Electrochemistry of Ordered Interfaces (#282/09237227 and 10131228)" from the Japanese Ministry of Education, Science, Sports and Culture.

References and Notes

(1) *Polymer Electrolyte Reviews 1* and *2*; MacCallum, J. R., Vincent, C. A., Eds.; Elsevier: London, 1987 and 1989.
(2) Gray, F. M. *Solid Polymer Electrolytes*; VCH Publishers: New York, 1991.
(3) *(3)Application of Electroactive Polymers*; Scrosati, B., Ed.; Chapman & Hall: London, 1993.
(4) Pei, Q.; Yang, Y.; Yu, G.; Zhang, C.; Heeger, A. J. *J. Am. Chem. Soc.* **1996**, *118*, 3922.
(5) Watanabe, M.; Ogata, N. In *Polymer Electrolyte Reviews 1*; MacCallum, J. R., Vincent, C. A., Eds.; Elsevier: London, 1987; Chapter 3, p 39.
(6) Watanabe, M.; Nishimoto, A. *Solid State Ionics* **1995**, *79*, 306.
(7) Watanabe, M.; Kanba, M.; Nagaoka, K.; Shinohara, I. *J. Polym. Sci., Polym. Phys.* **1983**, *21*, 939.
(8) Abraham, K. M.; Alamgir, M. *J. Electrochem. Soc.* **1990**, *137*, 1657.
(9) Peramunage, D.; Pasquariello, D. M.; Abraham, K. M. *J. Electrochem. Soc.* **1995**, *142*, 1789.
(10) Motogami, K.; Kono, M.; Mori, S.; Watanabe, M. *Electrochim. Acta* **1992**, *37*, 1725.
(11) Kono, M.; Furuta, K.; Watanabe, M.; Ogata, N. *Polym. Adv. Technol.* **1993**, *4*, 85.
(12) Kono, M.; Hayashi, E.; Watanabe, M. *J. Electrochem. Soc.* **1998**, *145*, 1521.
(13) Marchese, L.; Andrei, M.; Roggero, A.; Passerini, S.; Prosperi, P.; Scrosati, B. *Electrochim. Acta* **1992**, *37*, 1559.
(14) Hawker, C. J.; Chu, F.; Pomery, P. J.; Hill, D. J. T. *Macromolecules* **1996**, *29*, 3831.
(15) Herogues, V.; Gnanou, Y.; Fontanille, M. *Macromolecules* **1997**, *30*, 4791.
(16) Kato, Y.; Watanabe, M.; Sanui, K.; Ogata, N. *Solid State Ionics* **1990**, *40/41*, 632.
(17) Watanabe, M.; Nagasaka, H.; Ogata, N. *J. Phys. Chem.* **1995**, *99*, 12294.
(18) Sloop, S. E.; Lerner, M. M. *J. Electrochem. Soc.* **1996**, *143*, 1292.
(19) Sloop, S. E.; Lerner, M. M.; Thomas, S. S.; Tipton, A. L.; Paull, D. G.; Stenger-Smith, J. D. *J. Appl. Polym. Sci.* **1994**, *53*, 1563.
(20) Sonntag, C. V.; Schuchmann, H.-P.; Schomburg, G. *Tetrahedron* **1972**, *28*, 4333.
(21) Cohen, M. H.; Turnbull, D. *J. Chem. Phys.* **1959**, *31*, 1164.
(22) Watanabe, M. *Netsu Sokutei* **1997**, *24*, 12 (in Japanese).
(23) Ue, M. *J. Electrochem. Soc.* **1994**, *141*, 3336.
(24) Ue, M. *J. Electrochem. Soc.* **1996**, *143*, L270.
(25) Webber, A. *J. Electrochem. Soc.* **1991**, *138*, 2586.
(26) Vallée, A.; Besner, S.; Prud'homme, J. *Electrochim. Acta* **1992**, *37*, 1579.
(27) Alloin, F.; Sanchez, J.-Y.; Armand, M. *Solid State Ionics* **1993**, *60*, 3.
(28) Bruce, P. G.; Vincent, C. A. *J. Electroanal. Chem.* **1987**, *225*, 1.
(29) Bruce, P. G.; Hardgrave, M. T.; Vincent, C. A. *J. Electroanal. Chem.* **1989**, *271*, 27.
(30) Lascaund, S.; Perrier, M.; Armand, M.; Prud'homme, J.; Kapfer, B.; Vallée, A.; Gauthier, M. *Electrochim. Acta* **1998**, *43*, 1407.

MA981436Q